frontiers | Frontiers in Physiology

TYPE Original Research
PUBLISHED 12 July 2024
DOI 10.3389/fphys.2024.1408531

OPEN ACCESS

EDITED BY
Zhanqi Zhao,
Guangzhou Medical University, China

REVIEWED BY
Yuxian Wang,
Fudan University, China
Carmen Silvia Valente Barbas,
University of São Paulo, Brazil

*CORRESPONDENCE
Giuseppe Miserocchi,
giuseppe.miserocchi@unimib.it

†These authors share first authorship

RECEIVED 28 March 2024
ACCEPTED 18 June 2024
PUBLISHED 12 July 2024

CITATION
Miserocchi G, Rezoagli E, Muñoz-Del-Carpio-Toia A, Paricahua-Yucra LP, Zubieta-DeUrioste N, Zubieta-Calleja G and Beretta E (2024), Modelling lung diffusion-perfusion limitation in mechanically ventilated SARS-CoV-2 patients. *Front. Physiol.* 15:1408531. doi: 10.3389/fphys.2024.1408531

Modelling lung diffusion-perfusion limitation in mechanically ventilated SARS-CoV-2 patients

Giuseppe Miserocchi[1*†], Emanuele Rezoagli[1,2†], Agueda Muñoz-Del-Carpio-Toia[3], Leydi Pamela Paricahua-Yucra[4], Natalia Zubieta-DeUrioste[5], Gustavo Zubieta-Calleja[5] and Egidio Beretta[1]

[1]Dipartimento di Medicina e Chirurgia, Università Milano-Bicocca, Monza, Italy, [2]Department of Emergency and Intensive Care, Fondazione IRCCS San Gerardo dei Tintori, Monza, Italy, [3]Vicerrectorado de Investigación, Escuela de Postgrado Universidad Católica de Santa María, Arequipa, Peru, [4]Unidad de Cuidados Intensivos, Hospital Nacional Carlos Alberto Seguin Escobedo, Arequipa, Peru, [5]High Altitude Pulmonary and Pathology Institute (HAPPI-IPPA), La Paz, Bolivia

This is the first study to describe the daytime evolution of respiratory parameters in mechanically ventilated COVID-19 patients. The data base refers to patients hospitalised in the intensive care unit (ICU) at Arequipa Hospital (Peru, 2335 m) in 2021. In both survivors (S) and non-survivors (NS) patients, a remarkable decrease in respiratory compliance was observed, revealing a proportional decrease in inflatable alveolar units. The S and NS patients were all hyperventilated and their $SatO_2$ was maintained at >90%. However, while S remained normocapnic, NS developed progressive hypercapnia. We compared the efficiency of O_2 uptake and CO_2 removal in the air blood barrier relying on a model allowing to partition between diffusion and perfusion limitations to gas exchange. The decrease in O_2 uptake was interpreted as diffusion limitation, while the impairment in CO_2 removal was modelled by progressive perfusion limitation. The latter correlated with the increase in positive end-expiratory pressure (PEEP) and plateau pressure (Pplat), leading to capillary compression, increased blood velocity, and considerable shortening of the air-blood contact time.

KEYWORDS

dead space, respiratory compliance, gas exchanges, diffusion limitation, perfusion limitation, alveolar pressure, lung distension, mechanical ventilation

1 Introduction

Respiratory failure can develop when lung disease forces a patient to unsuccessfully adapt his ventilatory response to ensure gas exchange. The management of severe lung diseases involving loss of function in the alveolar units remains a challenge in intensive care units. From a pathophysiological point of view, the critical issue is that the spreading of lung disease can lead to the progressive loss of specific morpho-functional features of the air-blood barrier that normally ensure gas diffusion (Rezoagli et al., 2022). The efficiency of gas exchange is based not only on the morphological integrity of the alveolar-capillary membrane but also on the functional coupling between the gas diffusion capacity and perfusion capacity. The importance of this coupling has recently been emphasised, providing additional information on facing a perturbation in gas exchange (Beretta

10.3389/fphys.2024.1408531

TABLE 1 Data for survivors (S) and non-survivors (NS) patients on the first day of admission in ICU.

Survivors															
n°	Weight	Crs	PEEP	Vt	%Lung dist at PEEP	Pplat	% Lung dist at Pplat	FIO_2	% $SatO_2$	PaO_2	$PaCO_2$	P/F	$\dot{V}E$	DP	VR
1	61.4	25	8	418	44	25	82	0.5	98	95	41	190	177.0	17	2.0
2	65.7	51	10	482	50	20	72	0.6	96	84	40	141	183.5	10	1.9
3	66.0	43	12	474	55	23	79	0.7	96	82	43	117	186.7	11	2.1
4	70.6	36	11	499	53	25	82	0.7	95	94	33	144	176.7	14	1.5
5	71.5	32	12	473	55	27	85	0.7	95	92	33	131	165.4	15	1.5
6	66.0	32	16	441	65	30	90	0.9	93	75	36	84	187.1	14	1.8
7	68.7	21	10	480	50	23	79	0.7	96	85	23	121	209.7	13	1.3
8	71.5	30	12	603	55	32	92	0.7	97	65	20	93	253.1	20	1.3
9	72.0	35	14	563	60	30	90	0.8	94	98	36	123	218.9	16	2.1
10	64.0	23	18	384	69	35	95	1.0	95	81	41	81	180.0	17	2.0
11	70.5	30	9	502	47	26	84	0.5	96	75	37	150	206.5	17	2.0
12	81.0	32	14	442	60	28	87	0.7	97	123	38	176	158.2	14	1.6
13	51.5	23	10	418	50	28	87	0.8	97	73	31	92	243.5	18	2.0
14	41.5	10	10	291	50	38	98	0.5	94	70	43	140	245.4	28	2.8
15	63.3	19	14	356	60	33	93	0.9	95	79	57	88	180.0	19	2.7
16	63.3	21	12	246	55	24	81	0.7	97	134	26	191	124.4	12	0.9
17	65.0	34	13	387	57	24	81	0.8	99	158	48	205	131.0	11	1.7
18	63.0	24	14	307	60	27	85	0.7	96	63	77	90	160.8	13	3.3
19	66.0	44	13	394	58	22	77	0.8	98	87	50	108	137.3	9	1.8
20	69.7	27	10	426	50	26	84	0.5	97	99	48	198	158.9	16	2.0
21	66.0	30	10	446	51	25	82	0.6	96	50	37	79	164.1	15	1.6
22	48.8	32	14	351	60	25	82	0.8	95	77	36	96	201.1	11	1.9
23	**73.2**	**45**	**14**	446	**60**	**24**	**81**	**0.9**	**93**	**83**	**22**	**92**	**158.5**	10	0.9
24	60.6	26	14	342	60	27	86	0.8	95	71	46	88	158.0	13	1.9
25	67.8	27	10	439	50	26	84	0.6	98	119	42	198	181.3	16	2.0
26	61.5	27	16	439	65	32	92	0.9	95	72	44	80	249.8	16	2.9
27	61.5	18	16	246	65	30	90	1.0	94	82	45	82	140.0	14	1.7
28	71.2	43	14	445	59	24	81	0.8	98	109	27	136	175.0	10	1.3
29	61.5	49	14	417	60	23	78	0.7	95	66	40	95	176.3	9	1.9
30	65.1	38	14	472	60	27	85	0.8	94	81	32	103	217.5	13	1.8
mean	**65**	**31**	**13**	**421**	**56**	**27**	**85**	**1**	**96**	**87**	**39**	**124**	**184**	**14**	**2**
SD	**7.6**	**10**	**2**	**81.9**	**5.9**	**4**	**5.8**	**0.1**	**2**	**23**	**11**	**41**	**35**	**3.9**	**0.5**
NON-SURVIVORS															
n°	Weight	Crs	PEEP	Vt	%Lung dist at PEEP	Pplat	% Lung dist at Pplat	FIO_2	% $SatO_2$	PaO_2	$PaCO_2$	P/F	$\dot{V}E$	DP	VR
31	64.1	37	14	484	60	27	85	0.8	87	52	33	65	226.5	13	2.0

(Continued on following page)

10.3389/fphys.2024.1408531

TABLE 1 (*Continued*) Data for survivors (S) and non-survivors (NS) patients on the first day of admission in ICU.

NON-SURVIVORS															
n°	Weight	Crs	PEEP	Vt	%Lung dist at PEEP	Pplat	% Lung dist at Pplat	FIO_2	% $SatO_2$	PaO_2	$PaCO_2$	P/F	$\dot{V}E$	DP	VR
32	60.9	52	14	413	60	22	77	0.9	95	99	39	116	203.4	8	2.1
33	78.0	34	12	475	55	26	84	0.8	94	76	37	95	170.5	14	1.7
34	73.2	43	15	478	62	26	84	0.9	95	78	38	87	195.9	11	2.0
35	61.4	21	16	354	65	33	93	1.0	96	72	45	76	190.3	17	2.3
36	58.7	37	12	447	55	24	81	0.7	95	174	34	249	213.1	12	1.9
37	61.0	14	11	315	52	33	93	1.0	86	56	35	56	185.9	22	1.7
38	61.0	20	14	377	60	33	93	0.9	90	58	40	64	185.4	19	2.0
39	64.0	19	12	368	55	31	91	0.7	94	82	32	118	149.5	19	1.3
40	63.0	22	14	381	60	31	91	0.9	96	84	45	93	181.4	17	2.2
41	79.0	19	14	336	60	32	92	1.0	96	81	80	81	153.1	18	3.3
42	**42.5**	**25**	**13**	272	**58**	**24**	**81**	**0.7**	**94**	**73**	**27**	**99**	**202.2**	11	1.5
43	61.5	36	14	364	60	24	81	0.9	93	85	62	94	171.6	10	2.8
44	52.4	14	16	296	65	37	97	1.0	88	42	31	42	158.1	21	1.3
45	43.3	35	13	347	58	23	79	0.7	96	74	37	114	224.4	10	2.2
46	57.8	25	14	361	60	29	88	0.7	99	89	32	127	187.4	15	1.6
mean	**61.4**	**28**	**14**	**379**	**59**	**28**	**87**	**0.8**	**93**	**80**	**40**	**99**	**187**	**15**	**2.0**
SD	**10.1**	**11.1**	**1.4**	64.5	**3.5**	**4.5**	**6.3**	**0.1**	**3.7**	**29.2**	**13.3**	**46.6**	**23.3**	**4.3**	**0.5**

Patients #23 and #42 (in bold) were selected as representative patients of the survivors (S) and non-survivors (NS) groups.
Respiratory compliance (Crs) is expressed in ml·cmH_2O^{-1}, Tidal Volume (Vt) in ml, minute ventilation ($\dot{V}E$) in ml·kg^{-1}·min^{-1}; Positive End-Expiratory Pressure (PEEP), Plateau pressure (Pplat), and driving pressure (DP) are expressed in cmH_2O; PEEP %lung distension and Pplat %lung distension are expressed as percent of vital capacity from the standard Pressure-Volume curve of the respiratory system (Agostoni and Mead, 1964); PaO_2, $PaCO_2$, and P/F are expressed in mmHg; FIO_2, and Ventilatory Ratio (VR) are pure numbers; %$SatO_2$ percent of arterial oxygen saturation. In bold, mean values ± Standard Deviation. t-test unpaired: no significant differences were found in comparing S vs. NS.

et al., 2019; Miserocchi et al., 2022; Miserocchi, 2023a). Based on our past work on the air blood barrier function, we have been invited to comment on a database of daytime evolution of respiratory parameters in mechanically ventilated SARS-CoV-2 patients. SARS-CoV-2 respiratory failure has led to a massive need for mechanical ventilatory support worldwide (Rezoagli et al., 2021). This study wishes to explore the impact of SARS-CoV-2 disease on the diffusion/perfusion function in mechanical ventilated patients.

2 Material and methods

This was a retrospective study based on data from adult COVID patients hospitalised in the intensive care unit (ICU) at Arequipa Hospital (Peru, 2335 m) in 2021. The study was conducted in accordance with the Declaration of Helsinki. Patient consent was waived owing to the observational nature of the study, and the Institutional Review Board of Arequipa Hospital approved the data collection. No patient identifiers were used in this study.

Patients with a clinical diagnosis of respiratory failure and with a positive confirmation at the PCR quantification of Sars-CoV2 infection by sample evaluation from airways (i.e., naso-pharingeal swabs, bronchoaspirate, bronchoalveolar lavage) were intubated according to Institution standard of care of the admitting Intensive Care Unit and were enrolled in the current analysis. No specific exclusion criteria were considered. Settings of mechanical ventilation were applied in accordance to the recommendations of protective mechanical ventilation as reported in the ARDS guidelines (Fan et al., 2017).

All patients were maintained in the supine position, 30° head up (Spooner et al., 2014). The following parameters were collected daily during mechanical ventilation in ICU: tidal volume (Vt), respiratory rate (RR), minute ventilation ($\dot{V}E = Vt \cdot RR$) normalized to body weight ($\dot{V}E$/kg), positive end-expiratory pressure (PEEP), plateau pressure (Pplat), driving pressure (DP) calculated as Pplat-PEEP, FIO_2, $SatO_2$, arterial PaO_2, and $PaCO_2$. Reference values for PaO_2 and $PaCO_2$ at 2335 m are approximately 75 mmHg and 32.5 mmHg, respectively (Ramirez-Sandoval et al., 2016). P/F was calculated as the PaO_2 over FIO_2 ratio. Respiratory system compliance (Crs, ml ·

10.3389/fphys.2024.1408531

TABLE 2 Data for survivors (S) and non-survivors (NS) patients on the last day in ICU.

Survivors															
n°	Days in ICU	Crs	Vt	PEEP	%Lung dist at PEEP	Pplat	% Lung dist at Pplat	FIO_2	% $SatO_2$	PaO_2	$PaCO_2$	P/F	$\dot{V}E$	DP	VR
1	21	40	477	5	36	17	67	0.3	96	75	30	251	209.8	12	1.7
2	17	73	433	5	36	13	58	0.3	99	75	31	187	197.8	8	1.7
3	22	46	555	5	36	17	67	0.3	96	80	30	267	143.0	12	1.1
4	21	30	548	5	36	23	79	0.4	95	79	38	198	186.3	18	1.9
5	29	33	394	5	36	17	67	0.4	99	72	32	180	165.3	12	1.4
6	21	26	475	5	36	23	79	0.5	96	86	37	173	237.5	18	2.3
7	4	34	478	8	44	22	77	0.6	95	77	30	140	167.0	14	1.3
8	9	20	378	5	36	24	81	0.5	96	67	31	135	169.2	19	1.4
9	17	33	522	8	44	24	81	0.5	93	84	33	168	181.3	16	1.6
10	43	19	442	5	36	28	87	0.4	94	85	37	212	241.7	23	2.4
11	4	78	547	5	36	12	55	0.4	97	95	36	238	170.7	7	1.6
12	13	40	495	5	36	21	75	0.3	97	69	27	230	171.1	16	1.2
13	33	19	514	5	36	32	92	0.4	96	66	45	164	269.5	27	3.2
14	11	16	257	5	36	23	79	0.4	95	72	22	180	167.2	18	1.0
15	38	15	460	5	36	36	96	0.4	96	90	45	225	181.7	31	2.2
16	4	21	288	5	36	19	71	0.4	94	87	24	218	81.9	14	0.5
17	5	40	554	5	36	19	71	0.4	96	85	41	211	204.6	14	2.2
18	9	16	410	5	36	30	90	0.5	95	73	42	146	169.2	25	1.9
19	7	38	574	5	36	20	73	0.5	94	62	31	124	208.7	15	1.7
20	4	32	532	7	40	23	79	0.4	94	76	37	189	160.2	17	1.6
21	50	18	405	5	36	27	85	0.5	96	79	40	157	191.5	22	2.0
22	10	29	401	5	36	19	71	0.4	95	62	38	173	221.6	14	2.2
23	**23**	**26**	486	**5**	**36**	**24**	**81**	**0.3**	**96**	**66**	**35**	**218**	**212.5**	**19**	**2.0**
24	12	30	393	5	36	18	69	0.4	96	73	38	169	155.6	13	1.6
25	4	30	507	5	36	22	77	0.4	96	101	30	253	291.6	17	2.3
26	5	131	590	8	43	12	55	0.4	96	72	34	168	193.2	5	1.8
27	17	32	422	5	36	18	69	0.4	96	83	23	208	178.4	13	1.1
28	4	23	475	5	36	26	83	0.4	95	91	33	227	173.5	21	1.5
29	12	46	458	8	44	18	69	0.5	95	70	38	156	178.7	10	1.8
30	20	56	558	5	36	15	62	0.4	95	84	43	209	171.4	10	2.0
mean	**16**	**36**	**468**$^{\#\#}$	**5**$^{\#\#}$	**37**$^{\#\#}$	**21**$^{\#\#}$	**75**$^{\#\#}$	**0.4**$^{\#\#}$	**96**	**78**$^{\#\#}$	**34**$^{\#\#}$	**192**$^{\#\#}$	**188**	**16**	**2**
SD	**12.3**	**23.5**	80.1	**1.0**	**2.9**	**5.6**	**10.3**	**0.07**	**1.3**	**9.7**	**6.1**	**37.2**	**39.1**	**5.9**	**0.5**
NON-SURVIVORS															
n°	Days in ICU	Crs	Vt	PEEP	%Lung dist at PEEP	Pplat	% Lung dist at Pplat	FIO_2	% $SatO_2$	PaO_2	$PaCO_2$	P/F	$\dot{V}E$	DP	VR
31	26	29	459	14	60	30	90	0.9	90	89	60	99	243.5	16	3.9

(Continued on following page)

10.3389/fphys.2024.1408531

TABLE 2 (*Continued*) Data for survivors (S) and non-survivors (NS) patients on the last day in ICU.

NON-SURVIVORS															
n°	Days in ICU	Crs	Vt	PEEP	%Lung dist at PEEP	Pplat	% Lung dist at Pplat	FIO_2	% $SatO_2$	PaO_2	$PaCO_2$	P/F	$\dot{V}E$	DP	VR
32	14	18	410	18	69	41	100	1.0	86	48	64	48	228.9	23	3.9
33	10	34	497	14	60	29	88	0.8	94	67	36	84	184.8	15	1.8
34	31	22	512	14	60	37	97	1.0	91	72	54	72	244.8	23	3.5
35	44	15	311	10	50	31	91	0.9	90	73	69	81	177.3	21	3.3
36	54	18	445	5	36	30	90	0.6	92	59	55	98	242.4	25	3.6
37	44	10	327	8	44	40	100	1.0	89	56	59	56	187.6	32	2.9
38	29	20	426	15	62	36	97	0.9	92	61	32	67	247.0	22	2.1
39	42	14	367	5	36	32	92	0.6	95	71	65	118	160.6	27	2.8
40	15	12	426	12	55	49	100	1.0	89	64	61	64	202.9	37	3.3
41	17	15	382	8	44	34	94	0.6	94	53	58	89	169.2	26	2.6
42	**27**	**9**	186	**14**	**60**	**34**	**94**	**1.0**	**75**	**56**	**100**	**56**	**153.2**	**20**	**4.1**
43	17	26	448	16	65	33	93	1.0	91	72	53	72	255.0	17	3.6
44	20	30	312	12	55	22	78	0.9	94	85	50	100	208.3	10	2.8
45	15	23	276	14	60	26	84	0.9	93	70	67	78	223.1	12	4.0
46	8	17	258	11	51	26	84	0.7	92	65	61	98	125.0	16	2.0
mean	**26**	**19**$^{**\#\#}$	**378****	**12****	**54****	**33**$^{**\#}$	**92**	**0.86****	**90***	**66****	**59**$^{**\#\#}$	**80****	**203**	**21**$^{**\#\#}$	**3.1**$^{**\#\#}$
SD	**13.9**	**7.5**	92.0	**3.8**	**9.8**	**6.6**	**6.7**	**0.16**	**4.7**	**10.9**	**15.0**	**19.3**	**39.5**	**7.2**	**0.7**

Patients #23 and #42 (in bold) were selected as representative patients of the survivors (S) and non-survivors (NS) groups.
Respiratory compliance (Crs) is expressed in ml·cmH_2O^{-1}, Tidal Volume (Vt) in ml, minute ventilation ($\dot{V}E$) in ml·kg^{-1}·min^{-1}; Positive End-Expiratory Pressure (PEEP), Plateau pressure (Pplat), and driving pressure (DP) are expressed in cmH_2O; PEEP %lung distension and Pplat %lung distension are expressed as percent of vital capacity from the standard Pressure-Volume curve of the respiratory system (Agostoni and Mead, 1964); PaO_2, $PaCO_2$, and P/F are expressed in mmHg; FIO_2, and Ventilatory Ratio (VR) are pure numbers; %$SatO_2$ percent of arterial oxygen saturation.
In bold mean values ± Standard Deviation. t-test paired:*$p < 0.05$ S vs. NS, **$p < 0.01$ S vs. NS*. t-test paired: $^{\#}$<0.05 first vs. last day ICU, $^{\#\#}p < 0.01$ first vs. last day ICU.

cmH_2O^{-1}) was calculated as the ratio Vt/(Pplat-PEEP). We derive % lung distension at PEEP and Pplat from the average Pressure-Volume curve of the respiratory system (Agostoni and Mead, 1964) and Ventilatory ratio ($\dot{V}_R$) defined as $\dot{V}_R = \frac{\dot{V}_{E measured} \cdot PaCO_{2measured}}{\dot{V}_{E predicted} \cdot PaCO_{2ideal}}$ where $\dot{V}_{E predicted}$ is calculated as body weight · 100 mL/min and $PaCO_{2ideal}$ is set at 37.5 mmHg (Sinha et al., 2013).

Statistics: descriptive data were reported as mean ± standard deviation; differences between continuous variables were reported as t-tests paired and unpaired as appropriate; correlations of continuous data were assessed by Pearson's correlation coefficient; alpha level<0.05 was deemed significant (two-tailed). All statistical analyses were performed using Microsoft Excel (Version 16.81).

3 Results

Table 1 reports data for survivors (S, n = 30; 26 males, 87%) and non-survivors (NS, n = 16; 15 males, 94%) patients referring to the first day of admission in ICU.

Table 2 reports data for S and NS patients referring to the last day of ICU.

Comparing data on the first and last days of ICU stay (Tables 1, 2) in S (n = 30) patients, we found the following:

- No significant change in Crs, but a significant decrease in PEEP and Pplat (with a corresponding decrease in lung distension);
- All subjects were hyperventilated relative to the standard value of 100 mL kg^{-1}·min^{-1}.
- Significant increase in diffusion/perfusion efficiency of the air–blood barrier for O_2 (increase in PaO_2, P/F, and decrease in FIO_2) and CO_2 (decrease in $PaCO_2$).

The same comparison for NS (n = 16) patients (Tables 1, 2) shows:

- Significant decrease in Crs with no change in PEEP and significant increase in Pplat (increase in lung distension).
- All subjects were hyperventilated.

10.3389/fphys.2024.1408531

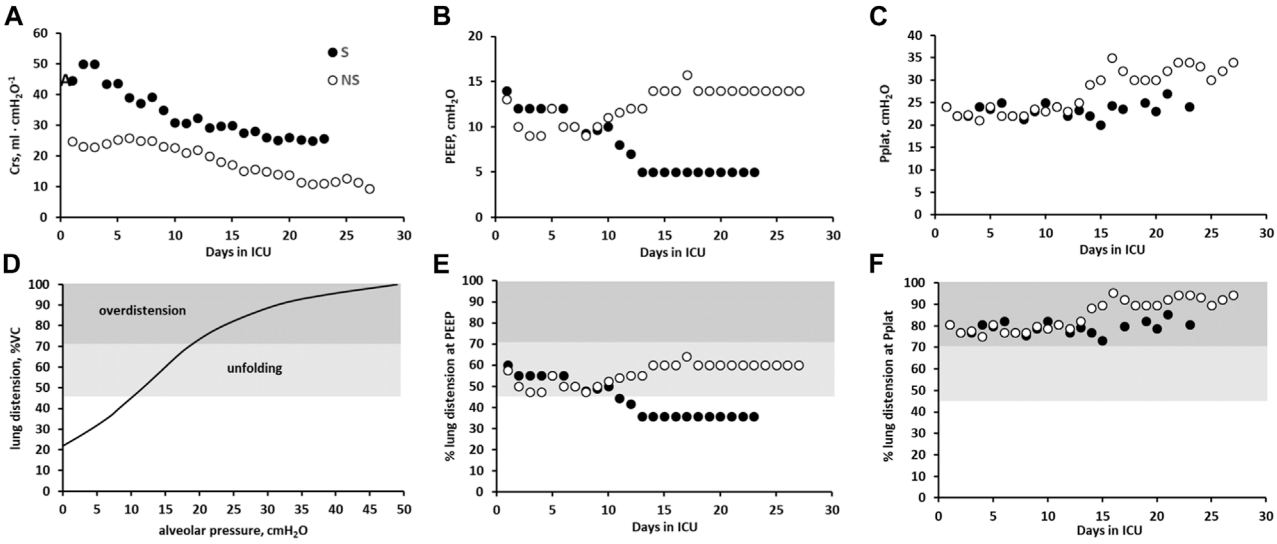

FIGURE 1
Respiratory parameters in 2 representative patients. Survivors (S, closed circles) and non-survivors (NS, open circles) in all panels. First row. Data referring to the time course of Crs **(A)**, PEEP **(B)**, and Pplat **(C)** Second row: Panel **(D)** reports the degree of lung distension based on the volume-pressure curve of the respiratory system in the supine position. Grey levels refer to the alveolar folding/unfolding and lung overdistension zones. Panels **(E,F)** report %lung distension for the two subjects at PEEP and Pplat, respectively.

- No change in diffusion/perfusion efficiency of the air–blood barrier for O_2 (PaO_2, P/F, and decrease in FIO_2), but a considerable reduction in diffusion/perfusion efficiency for CO_2 elimination (increase in $PaCO_2$).

Upon comparing data from the first day between the S and NS patients, no significant differences were found. However, the same comparison for the last day showed significant differences for all parameters considered, except ventilation, revealing a considerable loss of diffusion/perfusion efficiency of the air–blood barrier concerning O_2 and CO_2 and greater overdistension of the lung at both PEEP and Pplat.

We decided to discuss two representative patients from the S and NS groups (patient #23 and #42 in Tables 1, 2, respectively). Both patients showed a comparable decrease in Crs, with opposite fates concerning the diffusion/perfusion efficiency of the air-blood barrier for O_2 and CO_2.

3.1 Respiratory mechanics and alveolar pressure during mechanical ventilation

The first row in Figures 1A–C shows the time course of Crs, PEEP, and Pplat in two representative patients: survivors (S, closed symbols) and non-survivors (NS, open symbols). In both patients, Crs decreased over time to a similar extent, although the Crs values in NS were lower (Panel A). A clear dissociation is seen in panel B, as PEEP increased in NS while decreasing in S. Panel C reports the Pplat values that increased over time in NS but remained essentially steady in S.

Panel D in the second row of Figure 1 shows the pressure-volume relationship of the respiratory system (Agostoni and Mead, 1964), which is expressed as a percentage of the maximum. The maximum volume decreased with decreasing Crs, reflecting a decrease in inflatable alveolar units (IAU). If the mechanical properties of the residual IAU remained unchanged, the curve in Figure 1D reflects the *specific* compliance of the IAU. Based on this assumption, the ordinate can be used to express the corresponding degree of lung distension of the IAU as a function of the alveolar pressure. The light grey area includes the portion of the pressure-volume curve with the highest specific compliance, extending from 45% to 70% lung distension, corresponding to a range of alveolar pressures from approximately 10–20 cmH_2O. In this range of pressures, the process of unfolding of the alveolar surface takes place on inspiration, reflecting the existence of a "*reserve*" surface area of the corrugated alveolar cells (Weibel, 2015). As the unfolding process develops, the parenchymal stretch gradually increases (from the light to the darker grey area), indicating lung overdistension. Under physiological conditions at rest, an increase in tidal volume during spontaneous breathing is achieved by an increase in transpulmonary pressure of approximately 5 cmH_2O; accordingly, the same tidal volume in mechanical ventilation would be achieved by an alveolar pressure of approximately 5 cmH_2O, corresponding to 30% lung distension, well below the saturation of the unfolding zone. Panels E and F show the degree of lung distention at PEEP and Pplat, respectively, for the two subjects. In the case of NS, lung distension at PEEP falls in the light grey area, whereas at Pplat, lung distension falls in the overdistension zone for both patients.

3.2 Gas exchange

Panel A in Figure 2 shows that the time course of P/F significantly decreased in both patients. As shown in Panel B, no significant differences in $SatO_2$ were observed. Panels C and E again

10.3389/fphys.2024.1408531

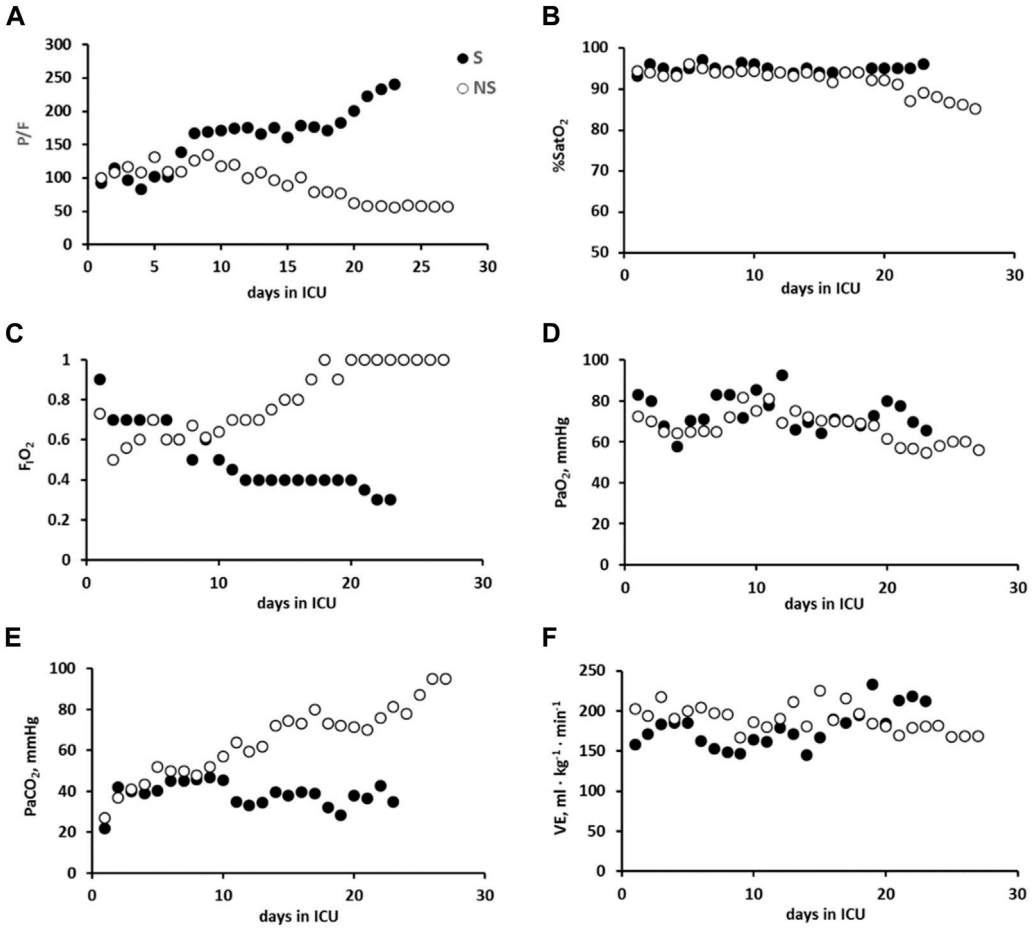

FIGURE 2
Data referring to the time course of gas exchange in the two representative patients: survivors, S (closed symbols), and non-survivors (NS, open symbols) in all panels.: P/F **(A)**, $SatO_2$ **(B)**, FIO_2 **(C)**, PaO_2 **(D)**, $PaCO_2$ **(E)**, and VE/kg **(F)**.

show a divergence in the time courses of FIO_2 and $PaCO_2$, despite displaying a similar time course for PaO_2 and VE/kg (Panels D and F, respectively).

Figure 3 (Panel A) shows the relationships of P/F plotted vs. Crs; for a decrease in Crs, P/F increased in patient S but decreased in NS. Panel B shows a decrease in P/F with increasing PEEP in patient NS; conversely (Panel C), P/F increased in S with decreasing PEEP.

Figure 4 shows the time course of tidal volume (Vt) and respiratory rate (RR) in S and NS patients (Panels A and B). By decreasing PEEP (Figure 1B), a higher driving pressure can increase Vt in S patient. Conversely, the opposite occurred in NS patient due to an increase in PEEP (Figure 1B), particularly considering the greater decrease in lung compliance (Figure 1A). Furthermore, it should be noted that in NS patients, the Vt approaches the anatomical dead space. The RR (Panel B) remained high for both subjects.

Concerning the ventilatory ratio, a clear dependence on ventilation is observed, albeit in opposite directions, considering S and NS patients (panel C). Panel D shows the striking dependence of the ventilatory ratio on $PaCO_2$; in the case of patient S, PaCO2 remained within the physiological range, while it increased remarkably in patient NS.

4 Discussion

To our knowledge, this is the first study to compare the evolution of respiratory parameters in survivors and non-survivors mechanically ventilated SARS-CoV-2 patients hospitalised in ICU. This is a physiologic study and not a clinical study with the ambition of a validation phase of the results. The novelty is the longitudinal physiological data granularity, the stratification by outcome. The data interpretation is made on physiological models that offer a mechanistic reading to the ventilatory data and gas exchange behaviour in patients who did or did not survive at ICU discharge. We will discuss the differences defining a computational biophysical model allowing to define potential diffusion/perfusion limitations of alveolar gas exchanges.

Figure 5 summarises the various conditions that may impact gas exchange at the alveolar level during the development of lung diseases, such as SARS-CoV-2 infection. Diffusion limitation may progress from a physiological condition (A) to interstitial oedema (B) and severe oedema with alveolar flooding (C). The development of oedema reflects an increase in microvascular permeability due to the progressive fragmentation of the proteoglycan component of the interstitial macromolecular network (Negrini et al., 1998; Negrini

10.3389/fphys.2024.1408531

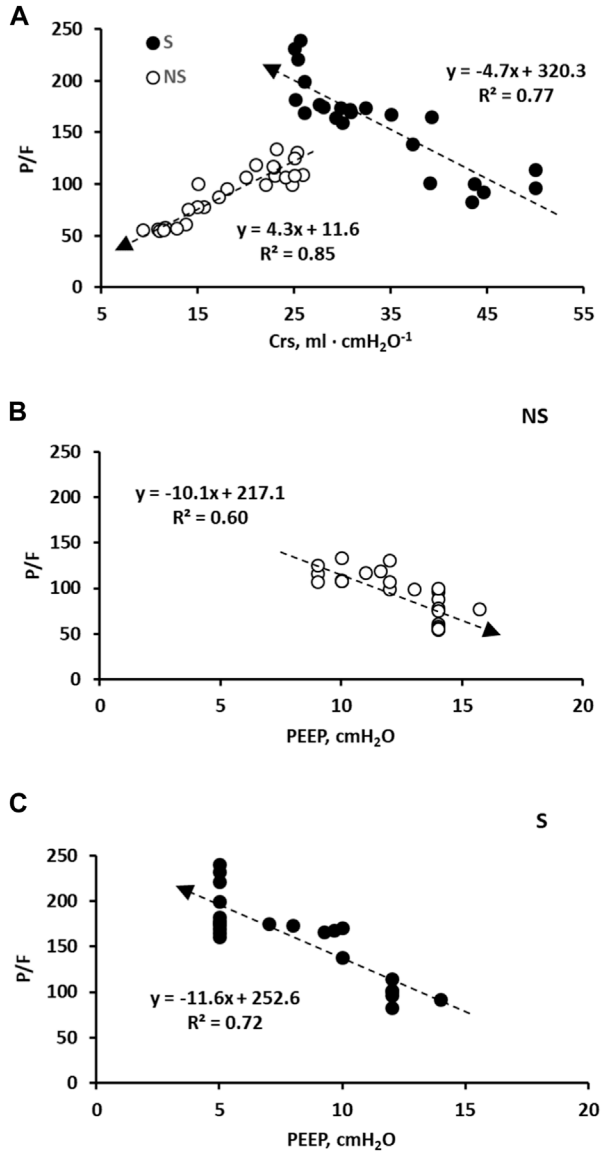

FIGURE 3
(A): correlation between day-time P/F vs. Crs in the two subjects S (closed symbols) and NS (open symbols). **(B)**: correlation between day-time P/F vs. PEEP in subject NS. **(C)**: correlation between day-time P/F vs. PEEP in subject S. Time dependence is expressed by the arrows in all panels.

et al., 2008; Moriondo et al., 2012; Yi et al., 2016). The path from A to C indicates a progressive increase in the shunt effect. The path from A to E shows a case of perfusion limitation due to pulmonary capillary squeezing due to lung overdistension (D) or complete vessel closure due to thrombosis (E). The progression from A to D led to an increase in dead space. Red dashed arrows indicate mixed events that occur in severe lung pathology.

We interpret the decrease in *Crs* as mainly due to the loss of inflatable alveolar units (IAU) during disease progression and partly due to the increase in tissue elastance during the development of interstitial oedema (Dellacà et al., 2008). Gas exchange can occur only in the IAU, which retains its morphofunctional features to ensure gas diffusion.

4.1 Dependence of Vc on lung distension

An increase in alveolar pressure leads to a decrease in capillary blood volume (*Vc*), owing to the squeezing of capillaries (Figure 5D) caused by an increase in parenchymal stretching (Glazier et al., 1969; Brower et al., 1985; Nieman et al., 1988; Koyama and Hildebrandt, 1991; Miserocchi et al., 2008). This decrease was found to vary remarkably among subjects, depending on the individual morphofunctional assembly of the alveolar capillary unit. The latter is characterised by the ratio of *Vc* to the diffusion capacity of the alveolar membrane (*Vc/Dm*), which essentially compares inter-individual differences in the extension of the pulmonary alveolar capillary network to the alveolar size (Miserocchi et al., 2008). The present available data do not allow for the estimation of inter-individual differences in *Vc/Dm* among patients. Accordingly, Figure 6 shows three cases of *Vc* ranging at Functional Residual Capacity (FRC) from 150 to 300 mL (corresponding to different *Vc/Dm* ratios). The figure reports the expected decrease in *Vc* with increasing lung distension with a PEEP of 5 and 15 cmH_2O (Miserocchi et al., 2008): clearly, the decrease in *Vc* (in absolute terms) is larger the greater the *Vc* value at FRC (Figure 5D).

Interestingly, a decrease in pulmonary blood volume has been documented in post COVID-19 through Dual-energy CT scan not only in opacification areas but also in parenchyma of normal appearance in acute (Aydin et al., 2021; Ball et al., 2021) and post-acute phase (Mohamed et al., 2023) (Figure 5E), suggesting a potential limitation to perfusion.

4.2 Gas exchange

We have developed a model to estimate the dependence of alveolar gas exchange resulting from the functional coupling of blood capillary flow with gas diffusion flows (Beretta et al., 2019; Miserocchi et al., 2022; Miserocchi, 2023b). Our present aim is to rely on this model to compare two distinct conditions: hyperoxia and normocapnia in S patients, against hyperoxia and hypercapnia in NS patients. We shall briefly summarize the principles of the biophysical model.

Based on the gas mass conservation notion (Piiper and Scheid, 1981) and an exponential kinetics of the equilibration process, the alveolar-capillary equilibration for gas exchange reached at the exit of the blood from the capillary is mathematically defined as:

$$L_{eq} = e^{-\frac{Tt}{\tau}} \quad (1)$$

being *Tt* blood capillary transit time (also known as "*capillary residence time*" or "*blood contact time*"), and τ is the time constant of the exponential kinetics. *Tt* is the key parameter to switch from volumes to flows and can be estimated as the ratio of pulmonary blood capillary volume (*Vc*) to cardiac output ($\dot{Q}$):

$$Tt = \frac{Vc}{\dot{Q}} \quad (2)$$

The kinetics of the equilibration is defined by the time constant given by:

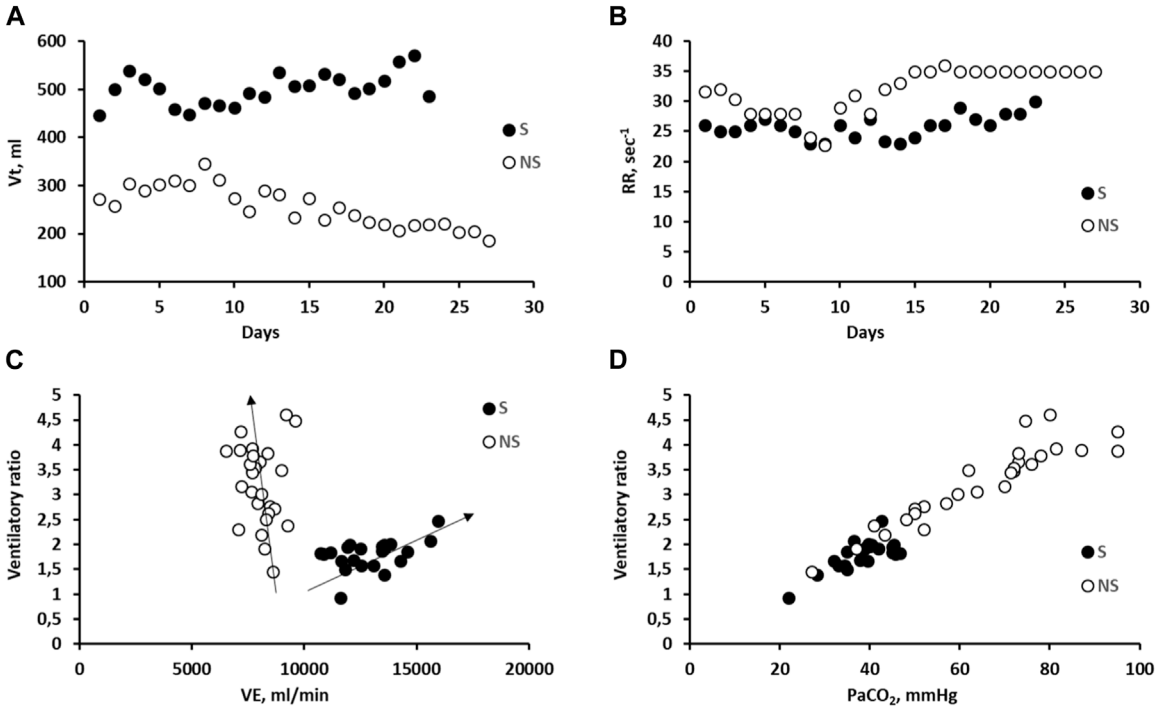

FIGURE 4
(A): correlation between tidal volume (Vt) vs. days in subjects S and NS; **(B)**: correlation between respiratory rate (RR) vs. PEEP in subjects S and NS. **(C)**: correlation between day-time Ventilatory ratio vs. Ventilation (VE) in the two representative subjects S and NS. **(D)**: correlation between day-time Ventilatory ratio vs. $PaCO_2$ in the two representative subjects S and NS.

$$\tau = \frac{\beta Vc}{DO_2} \text{ for } O_2 \quad (3)$$

and

$$\tau = \frac{\alpha Vc}{DCO_2} \text{ for } CO_2 \quad (4)$$

being DO_2 and DCO_2, the respective diffusive capacities, while β and α include gas solubility and transport capacity in blood.

Leq can vary from 0 (perfect equilibration) to 1 (total lack of equilibration) (Beretta et al., 2019; Miserocchi et al., 2022; Miserocchi, 2023b).

This approach provided supplementary information to the classic $\dot{V}_A/\dot{Q}$ distribution (Wagner, 2008; Glenny and Robertson, 2011; Hopkins, 2020). Defining the kinetics of gas exchange equilibration that includes the estimate of the blood capillary transit time allows to develop the concept of "*shunt-like effect*" reflecting the decrease in $\frac{Vc}{Q}$ ratio. The latter was found to vary considerably among subjects, reflecting the heterogeneity (Miserocchi et al., 2008; Miserocchi, 2023b) of inborn morpho-functional arrangement of the air blood barrier as well as the individual response to functional conditions (lung stretching, hypoxia, increase in oxygen demand) (Miserocchi and Beretta, 2023).

4.3 Diffusion and perfusion limitation

The key issue on comparing S with NS is that both groups had a $SatO_2$>90%; however, while the former remained normocapnic, the latter developed hypercapnia.

Diffusion limitation is a specific case occurring for oxygen, due to its low solubility-diffusion coefficients (Eq. 3).

Figure 7 shows that under physiological conditions, *Leq* = 0 at the exit of the pulmonary capillaries.

The development of interstitial and severe alveolar edema (Figures 5B, C) represent the obvious case of diffusion limitation for O_2 uptake, due to the decrease in DO_2. As shown in Figure 7, an exponential loss of equilibration capacity occurred with a 5-times decrease in DO_2, compatible with the observed average decrease in *Crs* in patients relative to a physiological value of approximately 100 mL/cmH_2O. The loss of O_2 equilibration capacity for the whole lung simulates a "*shunt-like effect.*"

Oxygen diffusion limitation is commonly compensated for by an increase in F_IO_2. One shall report that for FIO_2 > 0.7 (Aggarwal et al., 2018), cellular (Kistler et al., 1967; Weibel, 1971) and tissue (Chow et al., 2003; Kallet and Matthay, 2013) damage in the lungs were reported, leading to increased alveolar permeability (Matalon and Egan, 1981; Kolliputi et al., 2010).

Conversely, a diffusion limitation is hardly conceivable for CO_2 exchange considering its high solubility-diffusion coefficients. Accordingly, one can develop the hypothesis of perfusion limitation.

The aim of our study is to find a cause-effect relationship for developing hypercapnia. Figure 8 presents a computational (Eq. 1) estimate of the exponential increase in perfusion limitation for CO_2 removal for Tt < 1 s by decreasing Vc (Eq. 2) (Figures 5D, E).

Besides a decrease in Vc due to pulmonary stretching, a further factor arises from tissue compression in developing oedema (Figures 5B, C), that could actually lead to complete vessel closure (Mazzuca et al., 2019), functionally equivalent to the case of thrombosis

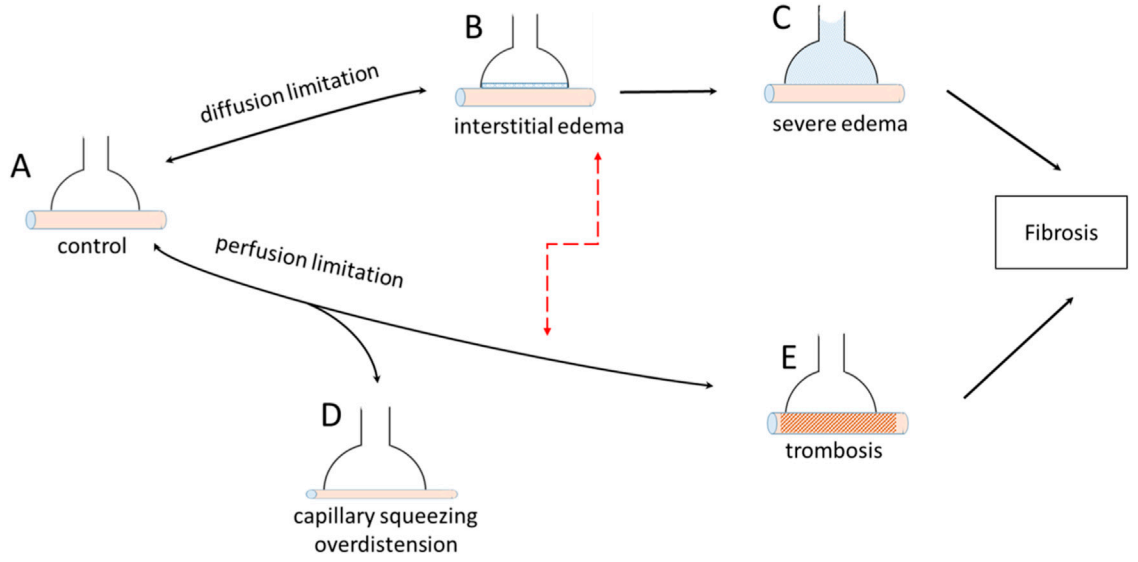

FIGURE 5
Various pathological conditions leading to diffusion limitation and perfusion limitation at the level of the air-blood barrier.

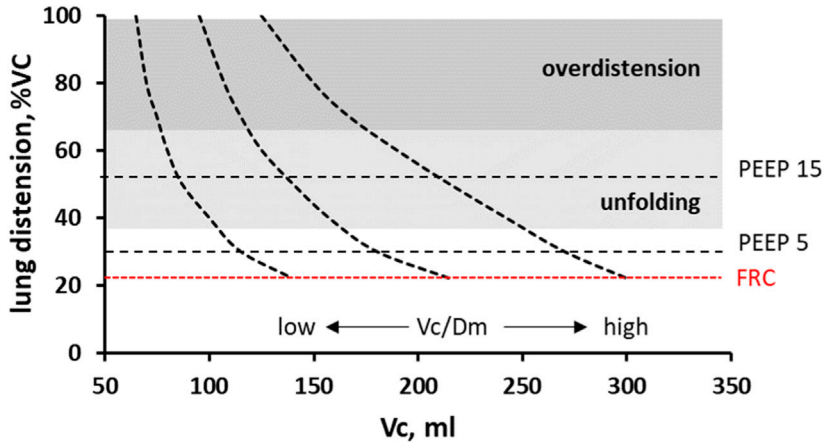

FIGURE 6
Decrease in capillary blood volume (Vc) on increasing lung distension, considering three cases of Vc values at Functional Residual Capacity (FRC) in the supine position. The Vc values correspond to either a low or high ratio to the diffusion capacity of the alveolar membrane (*Vc/Dm*), characterising inter-individual differences in alveolar morphology (from Miserocchi et al., 2008). Figure also refers to a PEEP of 5 and 10 cmH_2O.

(Figure 5E). Furthermore, studies on ECMO have confirmed that CO_2 removal is hampered by low blood flow (Karagiannidis et al., 2017; Giraud et al., 2021; Zanella et al., 2022).

4.4 Lung fluid balance

An estimate of the Starling pressure gradient controlling the lung fluid balance, particularly alveolar pressure, is presented in Figure 9. We accounted for the hydraulic and colloidal osmotic pressure, reflection coefficient, and alveolar surface tension (Beretta et al., 2021).

Data in Figure 9 show that, for Palv>5 cmH_2O, the transendothelial Starling gradient favours microvascular filtration and thus is an edemagenic factor (Miserocchi et al., 1993).

Lung overdistension has been found to increase microvascular filtration (Miserocchi et al., 1991), a finding confirmed by a computational model showing stress-dependent leak progression through an epithelial monolayer (Hamlington et al., 2016; Hamlington et al., 2018).

Notably, a decrease in Tt, resulting in an increase in blood velocity, leads to an increase in shear rate (Miserocchi et al., 2022), which in turn causes the increase in microvascular and protein permeability, thus favouring oedema (Sill et al., 1995;

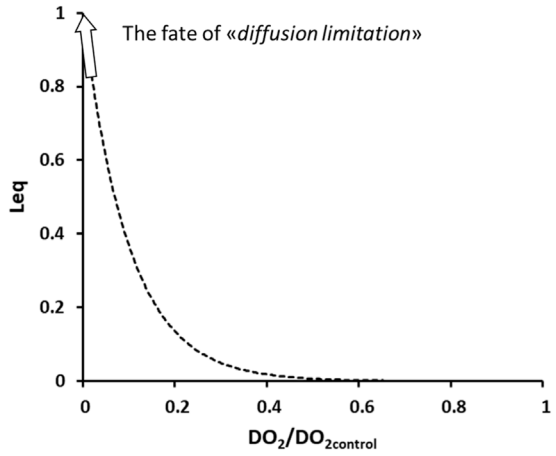

FIGURE 7
Exponential increase in *Leq* on decreasing diffusive capacitance for O_2 relative to control.

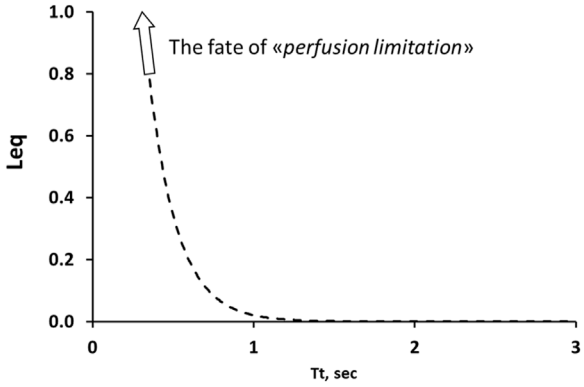

FIGURE 8
Computational model for cause-effect interpretation of perfusion limitation in CO_2 removal. Perfusion limitation expressed by the increase in Leq on decreasing Tt. Note the exponential increase in Leq for Tt < 1 s.

Lakshminarayanan et al., 2000; Mazzag et al., 2003; Barakat et al., 2006; Kang et al., 2014; Kolářová et al., 2014; Miserocchi and Beretta, 2023).

4.5 Study limitations

We have to acknowledge some study limitation. We did not have any specific exclusion criteria. However, we did not have information on the screening data of ICU admission, but this is a convenient sample size of patients admitted to ICU of the Arequipa Hospital in Perù with a clinical diagnosis of respiratory failure with a positive PCR confirmation of Sars-CoV2 infection that were enrolled from April 2020 to March 2021. This study is not designed to evaluate independent association of clinical variables on outcome by using multivariable models of association but aims at exploring the physiopathology of gas exchange in the air-blood barrier during acute respiratory failure. We relied on established computational physio-pathological models.

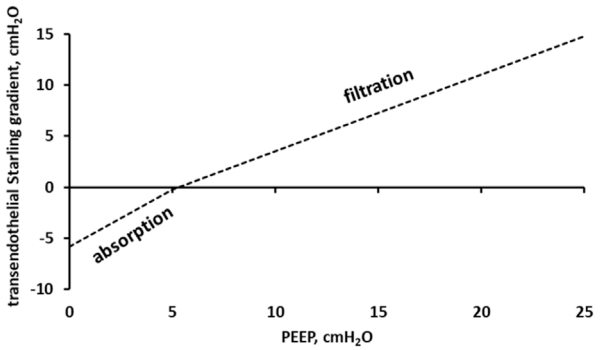

FIGURE 9
Starling pressure gradient across the lung capillary endothelium as a function of PEEP.

4.6 Concluding remarks

This paper deals with diffusion and perfusion limitation to alveolar gas exchanges in mechanically ventilated COVID-19 patients.

In the representative NS patient, P/F decreased in the first week of ICU stay (Figure 2A), clearly reflecting oxygen diffusion limitation compensated by an increase in PEEP and FIO_2 (Figures 1B, 2C, respectively). This was in accordance to the PEEP:FIO_2 tables (Brower et al., 2004) and the guidelines (Fan et al., 2017), the leading idea being to increase alveolar recruitment and ventilation to favor oxygen uptake, although a steady $SatO_2$>90%. However, the increase in PEEP may contribute to a progressive increase in $PaCO_2$ (Reazoagli and Bellani, 2022), due to perfusion limitation, hindering CO_2 removal (Figure 2E) and leading to a remarkable increase in the ventilatory ratio – which -in turn – is a marker *per se* of the respiratory failure severity (Figure 4D).

In representative S patient, the increase in P/F over the first week (Figure 2A) led to the decision (Brower et al., 2004) to decrease both PEEP and FIO_2 (Figures 1B, 2C). Consequently, this allowed ventilation of patient S with a progressively lower mean airway pressure, favoring CO_2 removal, notwithstanding the potential for alveolar de-recruitment.

In NS group, the ventilatory strategy led to $SatO_2$ >90% coupled with severe hypercapnia. The latter has been considered as a biomarker of increased dead space due to perfusion limitation, a condition associated independently with a high risk of mortality (Nuckton et al., 2002).

In fact, survivors or non-survivors are separated by a faint border considering that in both groups, lung compliance was decreased by the disease to approximately 1/5 of normal, meaning that the total number of alveolar units assuring gas exchange was decreased from a physiological value of approximately 500 (Ochs et al., 2004) to 100 million. One cannot exclude an overestimate of the decrease in *Crs* in the study population considering the possible presence of auto-PEEP, which may occur with an increasing respiratory rate (Marini,

2011). In severe cases of mechanically ventilated patients, a 70%–80% reduction in DLCO relative to the expected normal value was reported at 5–12 months (Krueger et al., 2023; van Willigen et al., 2023). Radiological pulmonary abnormalities have been described more than 100 days after the diagnosis of COVID-19 (Sonnweber et al., 2021). It appears reasonable to relate these decreased variables to pulmonary fibrosis development (Figure 5).

Several parameters obviously impact on the efficiency of gas exchanges in the air blood barrier.

The time dependent analysis that we performed allows an integrated view coherent with the parameters considered, highlighting the time dependence of gas exchanges in the air blood barrier, being diffusion limited for O_2 and perfusion limited for CO_2.

Data availability statement

The raw data supporting the conclusions of this article will be made available by the authors, without undue reservation.

Ethics statement

The requirement of ethical approval was waived by the Review Board of Arequipa Hospital for the studies involving humans because Data in the present paper refer to a retrospective study. The studies were conducted in accordance with the local legislation and institutional requirements. The ethics committee/institutional review board also waived the requirement of written informed consent for participation from the participants or the participants' legal guardians/next of kin because observational nature of the study.

Author contributions

GM: Conceptualization, Data curation, Formal Analysis, Investigation, Methodology, Project administration, Supervision, Visualization, Writing–original draft, Writing–review and editing. ER: Conceptualization, Data curation, Formal Analysis, Investigation, Methodology, Project administration, Supervision, Visualization, Writing–original draft, Writing–review and editing. AM-D-C-T: Data curation, Investigation, Resources, Writing–review and editing. LP-Y: Data curation, Investigation, Resources, Writing–review and editing. NZ-D: Data curation, Investigation, Resources, Writing–review and editing. GZ-C: Data curation, Investigation, Resources, Writing–review and editing. EB: Conceptualization, Data curation, Formal Analysis, Investigation, Methodology, Project administration, Supervision, Visualization, Writing–original draft, Writing–review and editing.

Funding

The author(s) declare that no financial support was received for the research, authorship, and/or publication of this article.

Conflict of interest

The authors declare that the research was conducted in the absence of any commercial or financial relationships that could be construed as a potential conflict of interest.

The author(s) declared that they were an editorial board member of Frontiers, at the time of submission. This had no impact on the peer review process and the final decision.

Publisher's note

References

Aggarwal, N. R., Brower, R. G., Hager, D. N., Thompson, B. T., Netzer, G., Shanholtz, C., et al. (2018). Oxygen exposure resulting in arterial oxygen tensions above the protocol goal was associated with worse clinical outcomes in acute respiratory distress syndrome. *Crit. Care Med.* 46, 517–524. doi:10.1097/CCM.0000000000002886

Agostoni, E., and Mead, J. (1964). "Statics of the respiratory system," in *Handbook of physiology respiration*. Editors W. O. Fenn and H. Rahn (Washington DC: American Physiological Society), 387–409.

Aydin, S., Kantarci, M., Karavas, E., Unver, E., Yalcin, S., and Aydin, F. (2021). Lung perfusion changes in COVID-19 pneumonia: a dual energy computerized tomography study. *Br. J. Radiol.* 94 (1125), 20201380. doi:10.1259/bjr.20201380

Ball, L., Robba, C., Herrmann, J., Gerard, S. E., Xin, Y., Mandelli, M., et al. (2021). Lung distribution of gas and blood volume in critically ill COVID-19 patients: a quantitative dual-energy computed tomography study. *Crit. Care.* 25 (1), 214. doi:10.1186/s13054-021-03610-9

Barakat, A. I., Lieu, D. K., and Gojova, A. (2006). Secrets of the code: do vascular endothelial cells use ion channels to decipher complex flow signals? *Biomaterials* 27 (5), 671–678. doi:10.1016/j.biomaterials.2005.07.036

Beretta, E., Grasso, G. S., Forcaia, G., Sancini, G., and Miserocchi, G. (2019). Differences in alveolo-capillary equilibration in healthy subjects on facing O2 demand. *Sci. Rep.* 9 (1), 16693. doi:10.1038/s41598-019-52679-4

Beretta, E., Romanò, F., Sancini, G., Grotberg, J. B., Nieman, G. F., and Miserocchi, G. (2021). Pulmonary interstitial matrix and lung fluid balance from normal to the acutely injured lung. *Front. Physiol.* 12, 781874. doi:10.3389/fphys.2021.781874

Brower, R., Wise, R. A., Hassapoyannes, C., Bromberger-Barnea, B., and Permutt, S. (1985). Effect of lung inflation on lung blood volume and pulmonary venous flow. *J. Appl. Physiol.* 58 (3), 954–963. doi:10.1152/jappl.1985.58.3.954

Brower, R. G., Lanken, P. N., MacIntyre, N., Matthay, M. A., Morris, A., Ancukiewicz, M., et al. (2004). Higher versus lower positive end-expiratory pressures in patients with the acute respiratory distress syndrome. *N. Engl. J. Med.* 351 (4), 327–336. doi:10.1056/NEJMoa032193

Chow, C. W., Herrera Abreu, M. T., Suzuki, T., and Downey, G. P. (2003). Oxidative stress and acute lung injury. *Am. J. Respir. Cell Mol. Biol.* 29, 427–431. doi:10.1165/rcmb.F278

Dellacà, R. L., Zannin, E., Sancini, G., Rivolta, I., Leone, B. E., Pedotti, A., et al. (2008). Changes in the mechanical properties of the respiratory system during the development of interstitial lung edema. *Respir. Res.* 9 (1), 51. doi:10.1186/1465-9921-9-51

Fan, E., Del Sorbo, L., Goligher, E. C., Hodgson, C. L., Munshi, L., Walkey, A. J., et al. (2017). An official American thoracic society/European society of intensive care medicine/society of critical care medicine clinical practice guideline: mechanical ventilation in adult patients with acute respiratory distress syndrome. *Am. J. Respir. Crit. Care Med.* 195 (9), 1253–1263. doi:10.1164/rccm.201703-0548ST

Giraud, R., Banfi, C., Assouline, B., De Charrière, A., and Bendjelid, K. (2021). Very low blood flow carbon dioxide removal system is not effective in a chronic obstructive pulmonary disease exacerbation setting. *Artif. organs* 45 (5), 479–487. doi:10.1111/aor.13867

Glazier, J. B., Hughes, J. M., Maloney, J. E., and West, J. B. (1969). Measurements of capillary dimensions and blood volume in rapidly frozen lungs. *J. Appl. Physiol.* 26 (1), 65–76. doi:10.1152/jappl.1969.26.1.65

Glenny, R., and Robertson, H. T. (2011). Distribution of perfusion. *Compr. Physiol.* 1 (1), 245–262. doi:10.1002/cphy.c100012

Hamlington, K. L., Bates, J. H. T., Roy, G. S., Julianelle, A. J., Charlebois, C., Suki, B., et al. (2018). Alveolar leak develops by a rich-get-richer process in ventilator-induced lung injury. *PloS one* 13 (3), e0193934. doi:10.1371/journal.pone.0193934

Hamlington, K. L., Ma, B., Smith, B. J., and Bates, J. H. (2016). Modeling the progression of epithelial leak caused by overdistension. *Cell. Mol. Bioeng.* 9 (1), 151–161. doi:10.1007/s12195-015-0426-3

Hopkins, S. R. (2020). Ventilation/perfusion relationships and gas exchange: measurement approaches. *Compr. Physiol.* 10 (3), 1155–1205. doi:10.1002/cphy.c180042

Kallet, R. H., and Matthay, M. A. (2013). Hyperoxic acute lung injury. *Respir. Care* 58, 123–141. doi:10.4187/respcare.01963

Kang, H., Cancel, L. M., and Tarbell, J. M. (2014). Effect of shear stress on water and LDL transport through cultured endothelial cell monolayers. *Atherosclerosis* 233, 682–690. doi:10.1016/j.atherosclerosis.2014.01.056

Karagiannidis, C., Philipp, A., Strassmann, S., Schäfer, S., Merten, M., and Windisch, W. (2017). Extracorporeal CO2 elimination (ECCO2R) for hypercapnic respiratory failure: from pathophysiology to clinical application. *Pneumologie* 71 (4), 215–220. doi:10.1055/s-0042-124406

Kistler, G. S., Caldwell, P. R., and Weibel, E. R. (1967). Development of fine structural damage to alveolar and capillary lining cells in oxygen-poisoned rat lungs. *J. Cell Biol.* 32 (3), 605–628. doi:10.1083/jcb.32.3.605

Kolářová, H., Ambrůzová, B., Svihálková Šindlerová, L., Klinke, A., and Kubala, L. (2014). Modulation of endothelial glycocalyx structure under inflammatory conditions. *Mediat. Inflamm.* 2014, 694312. doi:10.1155/2014/694312

Kolliputi, N., Shaik, R. S., and Waxman, A. B. (2010). The inflammasome mediates hyperoxia-induced alveolar cell permeability. *J. Immunol.* 184, 5819–5826. doi:10.4049/jimmunol.0902766

Koyama, S., and Hildebrandt, J. (1991). Air interface and elastic recoil affect vascular resistance in three zones of rabbit lungs. *J. Appl. Physiol.* 70 (6), 2422–2431. doi:10.1152/jappl.1991.70.6.2422

Krueger, T., van den Heuvel, J., van Kampen-van den Boogaart, V., van Zeeland, R., Mehagnoul-Schipper, D. J., Barten, D. G., et al. (2023). Pulmonary function three to five months after hospital discharge for COVID-19: a single centre cohort study. *Sci. Rep.* 13 (1), 681. doi:10.1038/s41598-023-27879-8

Lakshminarayanan, S., Gardner, T. W., and Tarbell, J. M. (2000). Effect of shear stress on the hydraulic conductivity of cultured bovine retinal microvascular endothelial cell monolayers. *Curr. Eye Res.* 21, 944–951. doi:10.1076/ceyr.21.6.944.6985

Marini, J. J. (2011). Dynamic hyperinflation and auto-positive end-expiratory pressure: lessons learned over 30 years. *Am. J. Respir. Crit. Care Med.* 184 (7), 756–762. doi:10.1164/rccm.201102-0226PP

Matalon, S., and Egan, E. A. (1981). Effects of 100% O2 breathing on permeability of alveolar epithelium to solute. *J. Appl. Physiol. Respir. Environ. Exerc. Physiol.* 50, 859–863. doi:10.1152/jappl.1981.50.4.859

Mazzag, B. M., Tamaresis, J. S., and Barakat, A. I. (2003). A model for shear stress sensing and transmission in vascular endothelial cells. *Biophys. J.* 84 (6), 4087–4101. doi:10.1016/S0006-3495(03)75134-0

Mazzuca, E., Aliverti, A., and Miserocchi, G. (2019). Understanding vasomotion of lung microcirculation by *in vivo* imaging. *J. Imaging* 5 (2), 22. doi:10.3390/jimaging5020022

Miserocchi, G. (2023a). Early endothelial signaling transduction in developing lung edema. *Life* 13 (6), 1240. doi:10.3390/life13061240

Miserocchi, G. (2023b). The impact of heterogeneity of the air-blood barrier on control of lung extravascular water and alveolar gas exchange. *Front. Netw. Physiol.* 3, 1142245. doi:10.3389/fnetp.2023.1142245

Miserocchi, G., and Beretta, E. (2023). A century of exercise physiology: lung fluid balance during and following exercise. *Eur. J. Appl. Physiol.* 123 (1), 1–24. doi:10.1007/s00421-022-05066-3

Miserocchi, G., Beretta, E., Rivolta, I., and Bartesaghi, M. (2022). Role of the air-blood barrier phenotype in lung oxygen uptake and control of extravascular water. *Front. Physiol.* 13, 811129. doi:10.3389/fphys.2022.811129

Miserocchi, G., Messinesi, G., Tana, F., Passoni, E., Adamo, S., Romano, R., et al. (2008). Mechanisms behind inter-individual differences in lung diffusing capacity. *Eur. J. Appl. Physiol.* 102 (5), 561–568. doi:10.1007/s00421-007-0625-2

Miserocchi, G., Negrini, D., Del Fabbro, M., and Venturoli, D. (1993). Pulmonary interstitial pressure in intact *in situ* lung: transition to interstitial edema. *J. Appl. Physiol.* 74 (3), 1171–1177. doi:10.1152/jappl.1993.74.3.1171

Miserocchi, G., Negrini, D., and Gonano, C. (1991). Parenchymal stress affects interstitial and pleural pressures in *in situ* lung. *J. Appl. Physiol.* 71 (5), 1967–1972. doi:10.1152/jappl.1991.71.5.1967

Mohamed, I., de Broucker, V., Duhamel, A., Giordano, J., Ego, A., Fonne, N., et al. (2023). Pulmonary circulation abnormalities in post-acute COVID-19 syndrome: dual-energy CT angiographic findings in 79 patients. *Eur. Radiol.* 33 (7), 4700–4712. doi:10.1007/s00330-023-09618-9

Moriondo, A., Marcozzi, C., Bianchin, F., Reguzzoni, M., Severgnini, P., Protasoni, M., et al. (2012). Impact of mechanical ventilation and fluid load on pulmonary glycosaminoglycans. *Respir. Physiol. Neurobiol.* 181 (3), 308–320. doi:10.1016/j.resp.2012.03.013

Negrini, D., Passi, A., De Luca, G., and Miserocchi, G. (1998). Proteoglycan involvement during development of lesional pulmonary edema. *Am. J. Physiol.* 274 (2), L203–L211. doi:10.1152/ajplung.1998.274.2.L203

Negrini, D., Passi, A., and Moriondo, A. (2008). The role of proteoglycans in pulmonary edema development. *Intensive Care Med.* 34 (4), 610–618. doi:10.1007/s00134-007-0962-y

Nieman, G. F., Paskanik, A. M., and Bredenberg, C. E. (1988). Effect of positive end-expiratory pressure on alveolar capillary perfusion. *J. Thorac. Cardiovasc. Surg.* 95 (4), 712–716. doi:10.1016/s0022-5223(19)35741-1

Nuckton, T. J., Alonso, J. A., Kallet, R. H., Daniel, B. M., Pittet, J. F., Eisner, M. D., et al. (2002). Pulmonary dead-space fraction as a risk factor for death in the acute respiratory distress syndrome. *N. Engl. J. Med.* 346 (17), 1281–1286. doi:10.1056/NEJMoa012835

Ochs, M., Nyengaard, J. R., Jung, A., Knudsen, L., Voigt, M., Wahlers, T., et al. (2004). The number of alveoli in the human lung. *Am. J. Respir. Crit. Care Med.* 169 (1), 120–124. doi:10.1164/rccm.200308-1107OC

Piiper, J., and Scheid, P. (1981). Model for capillary-alveolar equilibration with special reference to O2 uptake in hypoxia. *Respir. Physiol.* 46 (3), 193–208. doi:10.1016/0034-5687(81)90121-3

Ramirez-Sandoval, J. C., Castilla-Peón, M. F., Gotés-Palazuelos, J., Vázquez-García, J. C., Wagner, M. P., Merelo-Arias, C. A., et al. (2016). Bicarbonate values for healthy residents living in cities above 1500 meters of altitude: a theoretical model and systematic review. *High. Alt. Med. Biol.* 17 (2), 85–92. doi:10.1089/ham.2015.0097

Rezoagli, E., and Bellani, G. (2022). Monitoring lung injury severity and ventilation intensity during mechanical ventilation. *Crit. Care.* 23 (1), 412. doi:10.1186/s13054-019-2695-z

Rezoagli, E., Laffey, J. G., and Bellani, G. (2022). Monitoring lung injury severity and ventilation intensity during mechanical ventilation. *Semin. Respir. Crit. Care Med.* 43 (3), 346–368. doi:10.1055/s-0042-1748917

Rezoagli, E., Magliocca, A., Bellani, G., Pesenti, A., and Grasselli, G. (2021). Development of a critical care response - experiences from Italy during the coronavirus disease 2019 pandemic. *Anesthesiol. Clin.* 39 (2), 265–284. doi:10.1016/j.anclin.2021.02.003

Sill, H. W., Chang, Y. S., Artman, J. R., Frangos, J. A., Hollis, T. M., and Tarbell, J. M. (1995). Shear stress increases hydraulic conductivity of cultured endothelial monolayers. *Am. J. Physiol.* 268 (2), H535–H543. doi:10.1152/ajpheart.1995.268.2.H535

Sinha, P., Sanders, R. D., Soni, N., Vukoja, M. K., and Gajic, O. (2013). Acute respiratory distress syndrome: the prognostic value of ventilatory ratio--a simple bedside tool to monitor ventilatory efficiency. *Am. J. Respir. Crit. Care Med.* 187 (10), 1150–1153. doi:10.1164/rccm.201211-2037LE

Sonnweber, T., Sahanic, S., Pizzini, A., Luger, A., Schwabl, C., Sonnweber, B., et al. (2021). Cardiopulmonary recovery after COVID-19: an observational prospective multicentre trial. *Eur. Respir. J.* 57 (4), 2003481. doi:10.1183/13993003.03481-2020

Spooner, A. J., Corley, A., Sharpe, N. A., Barnett, A. G., Caruana, L. R., Hammond, N. E., et al. (2014). Head-of-bed elevation improves end-expiratory lung volumes in mechanically ventilated subjects: a prospective observational study. *Respir. Care* 59 (10), 1583–1589. doi:10.4187/respcare.02733

van Willigen, H. D. G., Wynberg, E., Verveen, A., Dijkstra, M., Verkaik, B. J., Figaroa, O. J. A., et al. (2023). One-fourth of COVID-19 patients have an impaired pulmonary function after 12 months of disease onset. *PloS one* 18 (9), e0290893. doi:10.1371/journal.pone.0290893

Wagner, P. D. (2008). The multiple inert gas elimination technique (MIGET). *Intensive Care Med.* 34 (6), 994–1001. doi:10.1007/s00134-008-1108-6

Weibel, E. R. (1971). Oxygen effect on lung cells. *Arch. Intern. Med.* 128, 54–56. doi:10.1001/archinte.1971.00310190058005

Weibel, E. R. (2015). On the tricks alveolar epithelial cells play to make a good lung. *Am. J. Respir. Crit. Care Med.* 191 (5), 504–513. doi:10.1164/rccm.201409-1663OE

Yi, E., Sato, S., Takahashi, A., Parameswaran, H., Blute, T. A., Bartolák-Suki, E., et al. (2016). Mechanical forces accelerate collagen digestion by bacterial collagenase in lung tissue strips. *Front. Physiol.* 7, 287. doi:10.3389/fphys.2016.00287

Zanella, A., Pesenti, A., Busana, M., De Falco, S., Di Girolamo, L., Scotti, E., et al. (2022). A minimally invasive and highly effective extracorporeal CO2 removal device combined with a continuous renal replacement therapy. *Crit. Care Med.* 50 (5), e468–e476. doi:10.1097/CCM.0000000000005428